



## OPEN ACCESS

EDITED BY  
Maria Angeles Esteban,  
University of Murcia, Spain

REVIEWED BY  
Jingguang Wei,  
South China Agricultural University,  
China  
Zhi Liao,  
Zhejiang Ocean University, China

\*CORRESPONDENCE  
Haiying Liang  
zjlianghy@126.com

<sup>†</sup>These authors have contributed  
equally to this work and share first  
authorship

SPECIALTY SECTION  
This article was submitted to  
Marine Fisheries, Aquaculture and  
Living Resources,  
a section of the journal  
Frontiers in Marine Science

RECEIVED 05 August 2022  
ACCEPTED 28 September 2022  
PUBLISHED 13 October 2022

CITATION  
Guo Z, Shen C, Liang H, Zhang M,  
Liang B and Zhang B (2022) Immune  
characterization and expression  
analysis of a goose-type lysozyme  
gene from *Pinctada fucata martensii*.  
*Front. Mar. Sci.* 9:1012323.  
doi: 10.3389/fmars.2022.1012323

COPYRIGHT  
© 2022 Guo, Shen, Liang, Zhang, Liang  
and Zhang. This is an open-access  
article distributed under the terms of  
the [Creative Commons Attribution  
License \(CC BY\)](#). The use, distribution  
or reproduction in other forums is  
permitted, provided the original  
author(s) and the copyright owner(s)  
are credited and that the original  
publication in this journal is cited, in  
accordance with accepted academic  
practice. No use, distribution or  
reproduction is permitted which does  
not comply with these terms.

# Immune characterization and expression analysis of a goose-type lysozyme gene from *Pinctada fucata martensii*

Zhijie Guo<sup>1†</sup>, Chenghao Shen<sup>1†</sup>, Haiying Liang<sup>1,2\*</sup>,  
Meizhen Zhang<sup>1</sup>, Bidan Liang<sup>1</sup> and Bin Zhang<sup>1</sup>

<sup>1</sup>Fisheries College, Guangdong Ocean University, Zhanjiang, China, <sup>2</sup>Guangdong Provincial Key Laboratory of Aquatic Animal Disease Control and Healthy Culture, Zhanjiang, China

In the present study, a g-type lysozyme was successfully screened and cloned from *Pinctada fucata martensii* (designated as *PmlysG*). The cDNA has a length of 973 bp with an open reading frame (ORF) of 769 bp, encoding a protein of 255 amino acids. The *PmlysG* transcript was detected in multiple tissues by quantitative real-time PCR (qRT-PCR), with the highest expression being in the hepatopancreas. Additionally, the temporal expression of *PmlysG* mRNA in the hepatopancreas after *in vivo* stimulation with pathogen-associated molecular patterns (PAMPs), such as lipopolysaccharide (LPS), peptidoglycan (PGN) and polyinosinic acid (PolyI:C) was detected by qRT-PCR. Although *PmlysG* responded to all three stimulation modes, it rapidly responded to PGN stimulation. Meanwhile, the recombinant protein of g-type lysozyme of *P.f. martensii* (rPmlysG) was used for antibacterial function analysis, and the results showed that rPmlysG has antibacterial function against *Vibrio parahaemolyticus*, *Aeromonas hydrophila*, and *Pseudomonas aeruginosa*. Overall, these study results suggest that the identified PmlysG participates in the innate immune responses of *P.f. martensii* against pathogen infection.

## KEYWORDS

*Pinctada fucata martensii*, g-type lysozyme, expression analysis, antibacterial activity, quantitative real-time PCR

## Introduction

Lysozyme, belonging to the GH (hydrolytic glycosidase [( $\beta$ -) glycoside hydrolase] subfamily 22, is a ubiquitous enzyme found in various organisms. It is a key effector molecule of the invertebrate and vertebrate innate immune systems. It can catalyze the hydrolysis of  $\beta$ -1,4-glycosidic linkage between N-acetylmuramic acid and N-acetylglucosamine alternating the sugar residues in the bacterial cell walls and peptidoglycan (PGN), thus inducing bacterial cell lysis (Jollès and Jollès, 1984; Prager

and Jollès, 1996). According to the source, structure, and physicochemical properties, lysozymes can be classified into six types: Goose-type-lysozyme (g-type); Invertebrate-type-lysozyme (i-type); Chicken-type-lysozyme (c-type); Bacterial lysozyme; Plant lysozyme and Bacteriophage lysozyme (Jiménez-Cantizano et al., 2008). Lysozyme exerts a synergistic effect on the cationic antimicrobial peptides exposed to the PGN layer of gram-negative bacteria (Hancock and Scott, 2000).

G-type lysozymes are mostly abundant in poultry eggs and were first identified in an antibacterial peptide of a white bird egg (Canfield and McMurry, 1967). In aquatic organisms, g-type lysozyme was first identified in *Paralichthys olivaceus* (Hikima et al., 2001). Besides, the g-type lysozyme has been identified in *Epinephelus coioides* (Yin et al., 2003), *Pseudosciaena crocea* (Zheng et al., 2007), and *Ctenopharyngodon idellus* (Ye et al., 2010). As a non-specific immune factor of fish, g-type lysozyme is closely related to the immune function of fish against bacterial infection. It is a natural endogenous antitoxin and helps improve the immunity of the body through its antibacterial, antiviral, and anti-inflammatory activities (Shakoori et al., 2019). For instance, g-type lysozyme significantly increased in different tissues of *C. idellus* after infection with *Aeromonas hydrophila* (Ye et al., 2010). Furthermore, the recombinant protein of g-type lysozyme induced by *Escherichia coli* poses antibacterial activity against various gram-negative and gram-positive bacteria in different environments (Li et al., 2008; Zhang et al., 2012).

Unlike advanced animals, mollusks are typical invertebrates without any unique immune system. In this regard, the innate immune factors play a crucial role in invertebrate immunity (Wang et al., 2013; He et al., 2019; He et al., 2020), including heme-mediated cellular and humoral immune responses (Fan et al., 2022; Lv et al., 2022). The innate immune factors dissolve the invading microorganisms or bacterial tissues using constitutive and inducible antibacterial molecules (Rolf and Siva-Jothy, 2003; He et al., 2018). Shellfish are filter-feeding organisms and are often exposed to various potential pathogens in the aquatic environment. Correspondingly, lysozyme in shellfish helps in pathogen defense due to its antibacterial effect and also helps in ingestion and digestion (Nilsen et al., 1999; Nilsen et al., 2003).

Recent studies have also identified the g-type lysozymes in invertebrates. For instance, the g-type lysozyme has been successfully identified in the adductor muscle of *Chlamys farreri* with active participation in immune response (Li et al., 2013). Similarly, a study has identified nine SNP sites and three ins-del polymorphic sites in the promoter region of G-type lysozyme of *Japanese scallops* (*Mizuhopecten yessoensis*). These mutations are classified into two haplotypes, which are associated with different transcription factor binding sites (He et al., 2012).

*Pearl oysters* (*Pinctada fucata martensii*) are one of the primary shellfish reared in the seawater pearls of southern China with high economic value (Wu et al., 2017a; Lu et al.,

2022). Nevertheless, several *P.f. martensii* have died in recent years due to environmental pollution (Qiu et al., 2014; Wu et al., 2017b). Thus, improving disease resistance in *P.f. martensii* has great significance.

In the present study, the cDNA sequence of goose-type lysozyme in *P.f. martensii* (*PmlysG*) was cloned using the rapid amplification of cDNA ends (RACE) technique and the expression of *PmlysG* in various tissues was analyzed using quantitative real-time PCR (qRT-PCR). Additionally, the *PmlysG* after treatment with pathogen-associated molecular patterns (PAMPs) were evaluated, including lipopolysaccharide (LPS), PGN, and polyinosinic acid (PolyI:C). Lastly, the recombinant protein of *PmlysG* (r*PmlysG*) was used against bacteria *in vitro* to further analyze the molecule characteristics of g-type lysozyme in *P.f. martensii*.

## Materials and methods

### Experimental materials and screening of immune effector molecules

*P.f. martensii* of approximately 2 years of age, with shell lengths of 5–6 cm, were collected directly from the sea in Chengwu, Zhanjiang, Guangdong Province, China. The *P.f. martensii* were cultured at 25–27°C in tanks with recirculating seawater for three days prior to experimentation.

The amino acid sequences with antimicrobial properties were obtained from the antimicrobial peptide database (APD3, <http://aps.unmc.edu/AP/main.php>), PubMed (<https://www.ncbi.nlm.nih.gov/pubmed/>), and National Center for Biotechnology Information (<https://www.ncbi.nlm.nih.gov/>). The genome data of *P.f. martensii* (Accession: PXD006786) (Du et al., 2017) was compared with the AMP database using a local reference. The gene sequences with the highest alignment rate were analyzed using the online blast in the NCBI protein sequence database to predict the types of immune effector molecules collected. A total of 21 sequences were obtained (Table S1). All the 21 sequences are interesting, some sequences have been studied and published in our previous study (He et al., 2020; Liang et al., 2022), other sequences are in study. One of the immune effector molecules identified as *PmlysG* was selected for follow-up studies in this manuscript.

### Characterization and cloning of *PmlysG*

The *PmlysG* specific primers for PCR amplification were designed using Primer Premier 5.0 (Table 1). The total RNA was obtained from *P.f. martensii* hemocytes using the Trizol reagent (Thermo-Fisher Scientific, USA). RNase-free DNase (Promega, USA) was used to avoid DNA contamination. The PCR product integrity was assessed on 1% agarose gel. The RNA

TABLE 1 Primers used in this study.

Primers	Sequence (5'-3')	Purpose
PmlysG-3'-inner	TGGGGAGACAACCATCATGCTT	3'fragment
PmlysG-3'-outer	GCATCGAAAACGAAGTAAAAT	3'fragment
PmlysG-5'-inner	ACTCCCAAAGAAATGCCCAACA	5'fragment
PmlysG-5'-outer	TGTCTCCCCATCCATTTCGTTGA	5'fragment
PmlysG-F	TGTTGGGCATTTCTTTGGCCAGC	Intermediate fragment
PmlysG-R	GTCTCCCCATCCATTTCGTTGA	Intermediate fragment
PmlysG-RT-F	TACCTTGTTGGGCATTTCTTTG	qRT-PCR
PmlysG-RT-R	TGGAGGGGATACAACACCGTCT	qRT-PCR
GAPDH-F	GCAGATGGTGCCGAGTATGT	qRT-PCR
GAPDH-R	CGTTGATTATCTTGGCGAGTG	qRT-PCR

concentration was determined based on the OD260/OD280 ratio using a NanoDrop 2000 spectrophotometer (Thermo-Fisher Scientific, USA). The cDNA was prepared using the Reverse Transcriptase M-MLV, following the manufacturer's protocol. The 3' and 5' ends of the PmlysG gene were cloned by RACE using the SMART RACE cDNA Amplification Kit (Clontech).

## Bioinformatics analysis

The homologous gene sequence was obtained through BLAST search. The open reading frame (ORF) was identified using the ORF finder. The theoretical isoelectric point and the molecular mass of the predicted amino acid sequence were estimated using ExPASy (<https://web.expasy.org/protparam/>). The signal peptide sequence was predicted using the SignalP4.0 server. The transmembrane domain analysis of sequences was conducted using TMHMMServer v.2.0 (<http://www.cbs.dtu.dk/services/TMHMM/>). The amino acid sequence and functional sites were predicted using SoftBerryPsite. The protein secondary structure was predicted using SOPAM.

The protein sequences of PmlysG and g-type lysozyme from six species (*Argopcten irradians*, *Mytilus galloprovincialis*, *Azumapcten farreri*, *Haliotis discus*, *Mizuhopecten yessoensis*, and *Phylla acuta*) were compared using DNAMAN6.0. Finally, the neighbor-joining phylogenetic tree was constructed using MEGA6.0.

## Tissue expression analysis

The relative expression level of PmlysG in various tissues of *P.f. martensii* was measured by quantitative real-time PCR. The tissues, including mantle, hemocytes, gonads, gills, hepatopancreas, and adductor muscle were obtained from 10 pearl oysters and immediately stored in liquid nitrogen for further use. The total RNA was extracted from the samples

according to a previously reported method (He et al., 2020). After obtaining the total RNA from various tissues, it was reverse transcribed into cDNA. Based on the obtained cDNA sequence, a pair of specific primers of PmlysG was designed using Primer Premier 5.0 (Table 1). The quantitative level of PmlysG in each tissue was detected through the premix and lightcycler96 real-time PCR system (Roche) according to a previously reported method (Liang et al., 2022).

The PmlysG transcript expression level in the hepatopancreas was quantified in terms of PAMPs, including LPS, PGN, PolyI:C to determine the possible role of PmlysG in immune responses. Healthy *P.f. martensii* (n = 320) samples were randomly divided into four groups (n = 80 per group), including LPS, PGN, PolyI:C, and PBS (control). The experimental groups (LPS, PGN, and PolyI:C) were injected with 100  $\mu$ L of LPS (10  $\mu$ g/mL), 100  $\mu$ L of PGN (10  $\mu$ g/mL), and 100  $\mu$ L of PolyI:C (10  $\mu$ g/mL), respectively. The control group was injected with 100  $\mu$ L of PBS. The mRNA expression levels of PmlysG were determined at 0, 3, 6, 9, 12, 24, 48, 72, and 96 hours after stimulation with PAMPs. The relative expression levels of the target genes were determined by the  $2^{-\Delta\Delta ct}$  method (Livak and Schmittgen, 2001), using GAPDH as the reference gene.

## Prokaryotic expression and purification

PCR fragment encoding the mature peptide of PmlysG was amplified using the specific primers PmlysGR and PmlysGF. The PCR product digested with M1uI/HindIII was subcloned into pET-28a (+) digested with the same enzymes to obtain the plasmid pET28a-PmlysG. The pET28a-PmlysG compound was verified through restriction enzyme digestion and DNA sequencing.

The recombinant plasmid pET28a-PmlysG was transferred into the BL21 (DE3) competent cells. An excellent single colony was inoculated in 4mL medium containing 50  $\mu$ g/mL of kanamycin. When the OD reached 0.6 ~ 0.8, the isopropyl-beta-D-thiogalactopyranoside (IPTG) was added to a final concentration of 0.5 mM, and then induced at 15°C and 37°C.

The fusion protein was purified using the HisBind purification kit (Pharmacia, Sweden), following the manufacturer's protocol.

## Antimicrobial assay

Several purified proteins were used against *Vibrio parahaemolyticus*, *Aeromonas hydrophila*, *Pseudomonas aeruginosa*, *Staphylococcus aureus*, *Micrococcus luteus*, *Bacillus subtilis*, and *Escherichia coli* to assess their antibacterial activities. Briefly, each bacterium was cultured in a 2216E liquid medium to the logarithmic growth phase. The bacterial solutions were centrifuged (3000 xg, 10 minutes), washed thrice using 1xPBS, and resuspended in PBS. The purified protein (50  $\mu$ L, 500  $\mu$ g/mL) was mixed and incubated with 50  $\mu$ L of each bacterial suspension at room temperature for 2 hours using PBS as a negative control. The mixture was then incubated at 37°C and the OD600 values at 0, 1, 2, 3, 4, 5, 6, 7, 8, 9, 10, 11, and 12 hours were measured using a microplate reader (EnSpire, PerkinElmer). Each experiment was conducted in triplicate.

## Transmission electron microscopy

Approximately 200  $\mu$ L of rPmlysG and 200  $\mu$ L of bacterial solution in the exponential growth period were mixed at 37 °C for 2 hours using PBS as the control. The mixture was centrifuged at 3000 rpm and room temperature for 10 minutes for deposition and then washed thrice with PBS to remove impurities. Later, 200  $\mu$ L of 2% sodium phosphotungstate aqueous solution was added to the bacterial suspension, which was then dropped on copper grids. The samples were air-dried after removing the residual water using filter paper for 5 minutes. Finally, the images were observed using a JEM-1230 JEM-1400 (Japan Electronics Corp) microscope under standard operating conditions.

## Statistical analysis

All experimental data were analyzed by One-way analysis of variance (ANOVAs) using SPSS 19.0 (IBM, USA). The differences between means were considered significant at  $P < 0.05$  and extremely significant at  $P < 0.01$ .

## Results

### Characterization of PmlysG

As depicted in Figure 1, the *PmlysG* cDNA is 973 bp long and contains a 3' untranslated region (UTR) of 121 bp and a 5' UTR of 84 bp. The *PmlysG* cDNA includes an ORF of 769 bp, encoding 255 amino acids. The predicted molecular mass of the PmlysG is 27.26 kDa, with an isoelectric point (pI) of 7.27. The highest hydrophobicity continuously appears from position 8,

with an index of 2.844. The highest hydrophilicity (hydrophilic protein) appears at position 198, with an index of -2.289 and an overall average coefficient of -0.306. The positively charged residue (Arg + Lys) is 15, and the negatively charged residue (ASP + Glu) is 15, indicating that *PmlysG* is a neutral charge.

The amino acids at positions 1-16 have a signal peptide (Supplementary Figure S1). The secondary structure predictions suggested that the active protein mainly contains random coils (51.70%), extended strands (12.94%),  $\alpha$ -helices (30.20%), and  $\beta$ -turn (5.49%). The domain analysis identified a single d153I\_ domain containing 176 amino acids (Supplementary Figure S2).

### Multiple sequence alignment and phylogenetic relationships

The alignment of PmlysG with the G-type lysozyme of other species indicated that PmlysG was similar to the g-type lysozyme in *Argopecten irradians* (60.5%), *Mytilus galloprovincialis* (58.74%), *Azumapecten farreri* (57%), and *Haliotis discus* (45.88%). The consistent similarity among the species reached 55.76% (Figure 2), based on which a phylogenetic tree was then constructed.

The phylogenetic tree classification of *PmlysG* showed that invertebrates and vertebrates formed a separate large branch. *P.f. martensii* shared the closest genetic relationship with *Argopecten irradians*, *Azumapecten farreri*, and *Mizuhopecten yessoensis* (Figure 3).

### Quantitative analysis of PmlysG in different tissues

The expression levels of *PmlysG* in the hepatopancreas, gonads, hemocytes, gill, adductor muscle, and mantle were analyzed using qRT PCR under normal physiological conditions. The *PmlysG* mRNA was ubiquitously expressed in various tissues, with significantly high expression in the hepatopancreas ( $P < 0.01$ ) (Figure 4).

### The mRNA expression of PmlysG after PAMPs stimulation

Compared with the control, the *PmlysG* mRNA expression rapidly increased in the hepatopancreas at 6 hours after LPS stimulation, reaching the maximum level at 72 hours ( $P < 0.01$ ), then it quickly returned to the normal level at 96 hours (Figure 5A). Moreover, *PmlysG* mRNA began to increase at 3 hours after PGN stimulation, reaching the maximum level at 6 hours ( $P < 0.01$ ), then decreased at 12 hours, increased at 24 hours, gradually decreased at 48 hours, and finally returned to the normal level (Figure 5B). However, after PolyI:C stimulation,

```

1  AAGCAGTGGTATCAACGCAGAGTACATGGGGAAAGTGATCACAAGTGTAGTTCTGAGAAT 60
61  ATCTTGATTCGGGTCAAGTTCATAGGGAGGAAAAATTTACTCCCAGCATGCTATCAATTC 120
                                     M L S I
121  TGCTTTTGTACCTTGTGGGCATTCTTTGGCCAGCGACGCACCGTGCAAAACTCCG 180
    L L F V T L L G I S L A S D A P C T N S
181  GTGGCCACTGTCAGGACGACCATGGTTCCTGTTCGGTAGCTACCACAGCCACCTGTGTT 240
    G G H C Q D D H G S C S G S Y H S H L C
241  CCGGTTCGGCTCACAGCGGTGTGTATCCCCTCCACATCTCCGGGTCTCACTCAGGAT 300
    S G S A H R R C C I P S T S S G S H S G
301  CTAGTTCTAGTGGTTATAATGCTATGGAGATGTACGAGCCTCCATCCCCTCCGACGTC 360
    S S S S G Y N C Y G D V T S L H P S G R
361  ACAGTGGAGAGTCGCCGCATCGCAAAACGAAGTAAAATATGACATATCTACCCTGAACG 420
    H S G G V A A S Q N E V K Y D I S T L N
421  CTCATAAAAGCTGCTACGTCACTGCCGGCAGGAACAAGTATCCATCCGGCCTTGATAG 480
    A H K S C Y V T A G R N N C I H P A L I
481  CTGCTTAGCCAGTAGAGAATCCCATGCTGGTCTGCTGCTACATTCAACGAATGGATGGG 540
    A A L A S R E S H A G R L L H S T N G W
541  GAGACAACCATCATGCTTATGGAGTACTCCAGTGTGACGTCGGTACTGCCCGTTTGT 600
    G D N H H A Y G V L Q C D V R Y C P V C
601  CCCATGGACTGAAGTGTACGACCTACGGATGGGATTCTTGTCAACATATTGATATGATGA 660
    S H G L K C T T Y G W D S C Q H I D M M
661  CCAAATACGTATTGGTCCCCTATATAAAAACAAGTCAAAGGAAACATCCCACTTGGCCGG 720
    T K Y V L V P Y I K Q V Q R K H P T W P
721  CCGTTCATCAGATGCAAGGAGCGTGGCTGCTTACAATTTGGACCAGGAAATGTGCAGT 780
    A A H Q M Q G G V A A Y N F G P G N V Q
781  CATGGGGTGGACTGGATATAGGAAGCACTGGAACGACTACAGCAATGACGTCATTGCCG 840
    S W G G L D I G S T G N D Y S N D V I A
841  GAGCACAGTATTGATCTCGCATGAAGGATGTAATAATGATGAACTGTAAAATGAAA 900
    R A Q Y L I S H E G W *
901  ATATCGAATAAAAGTGAAGTATTTTAATAATATGTCGTAATCTTTAAAAGCGCGAAG 960
961  TAAACCTAAAAAAAAAAAAAAAAAAAAAAAAAAAAAAAAA 996

```

FIGURE 1

A cDNA sequence and predicted amino acid sequence of *PmlysG*. Red font indicates start codon and stop codon, the straight line indicates signal peptide, and the shaded portion shows the d153L<sub>1</sub> domain.

*PmlysG* mRNA did not change in the first 12 hours, but began to rise at 24 and 48 hours, reaching a maximum at 72 hours ( $P < 0.05$ ), then began to decline after 72 hours (Figure 5C).

## Induced expression and purification of the *PmlysG*

The digested *PmlysG* gene fragment was about 1570 bp (Figure 6A). The successful construction of vector pET28-*PmlysG* was verified through sequencing. Further validation showed that 26.52 KDa protein was present in the recombinant bacteria but not in the negative control.

Moreover, no target bands were found in lanes 3 and 4 of the supernatant at 15 °C and 37 °C. However, clear target bands appeared in lanes 1 and 2 (whole bacteria), 5 and 6 (precipitation) of the experimental groups at 15 °C and 37 °C (Figure 6B). Western blot further verified the 27 kDa clear single staining bands, and the positions of the lanes were consistent with the above positions. Further analysis showed that the recombinant protein induced at 15 °C (lane 5) was brighter than the one induced at 37 °C (lane 6) (Figure 6C). These results indicate that the product is mainly expressed as an inclusion body, it was dialyzed, renatured, and transferred to a soluble buffer (PBS, 10% glycerol, 1 mL arginine, pH 7.4).

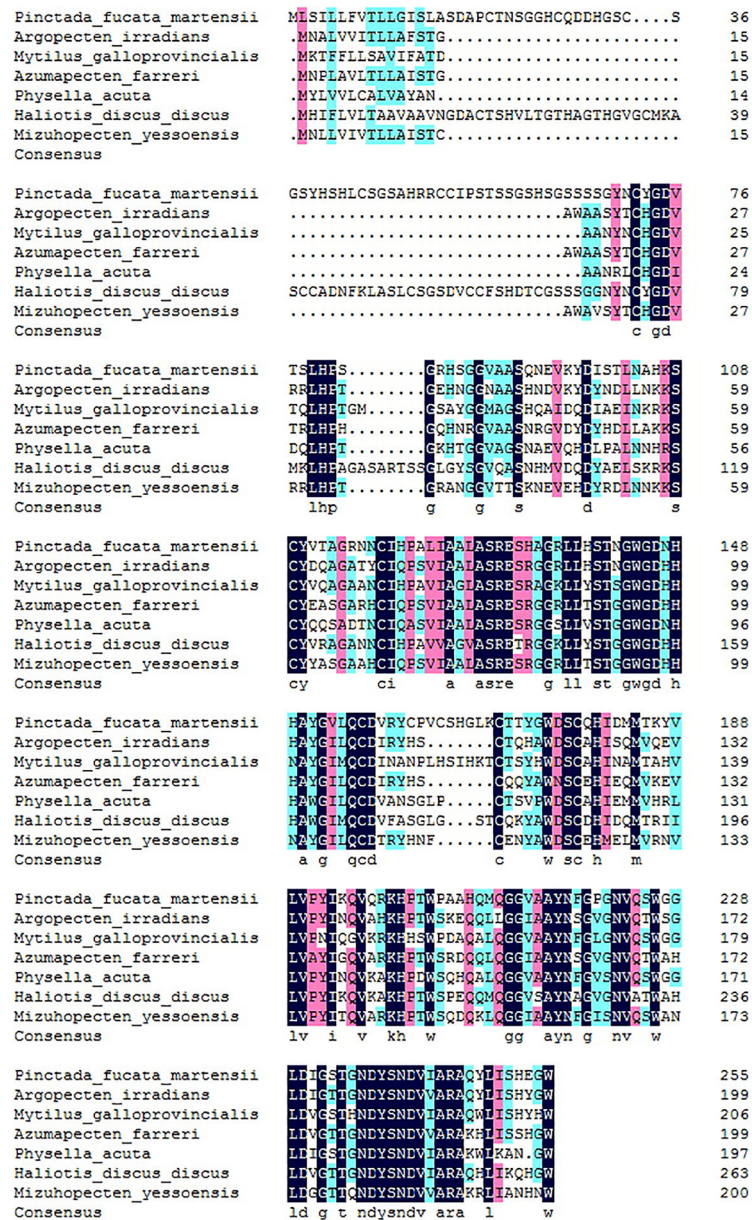


FIGURE 2  
*PmysG* Homology alignment and the coincident amino acids. Light blue and pink indicate that the similarity is more than 75% and 50%, respectively. Navy blue: Consensus amino acids.

### Antimicrobial activity

Seven bacteria, including three gram-positive bacteria and four gram-negative bacteria, were determined in the bacterial inhibition experiment. The purified protein (500 µg/mL) significantly inhibited the growth of gram-negative species (*V. parahaemolyticus*, *A. hydrophila*, and *P. aeruginosa*) ( $P < 0.05$ ) (Figure 7), but exhibited little effect on the growth of *S. aureus*, *M. luteus*, *B. subtilis*, and *E. coli* (Supplementary Figure S3).

### Transmission electron microscope observation

The morphological characteristics of *V. parahaemolyticus* and *A. hydrophila* after interacting with rPmysG were visualized using TEM to assess the antibacterial mechanism of g-type lysozyme in *P. f. martensii*. The exterior of the control *V. parahaemolyticus* (Figures 8A-C) was clear, and the contents were dense and uniform. The middle of *V. parahaemolyticus* shrank after

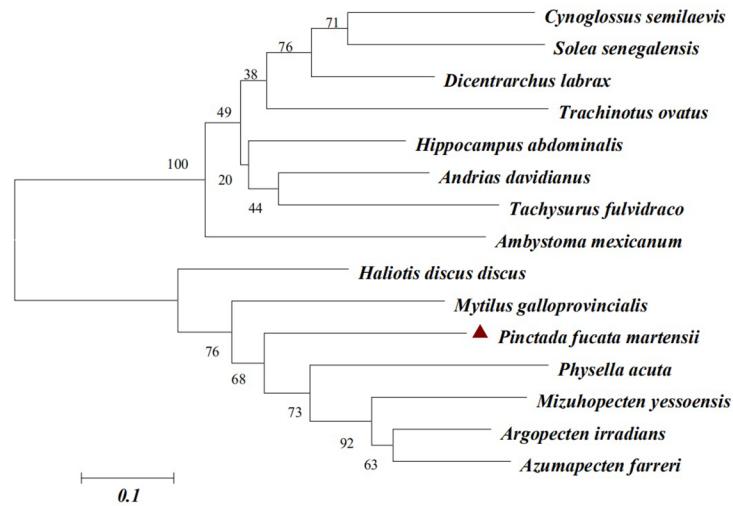


**FIGURE 3**  
 PmlysG Phylogenetic tree construction (Neighbor-joining method). GenBank accession numbers for some species are as follows: *Cynoglossus semilaevis* (AEQ19605.1), *Solea senegalensis* (CCA95109.1), *Dicentrarchus labrax* (AIE45885.1), *Tachysurus fulvidraco* (ALD84262.1), *Ambystoma mexicanum* (AEQ98812.1), *Haliotis discus* (AGQ50335.1), *Mytilus galloprovincialis* (AFQ35865.1), *Physella acuta* (ADV36303.1), *Mizuhopecten yessoensis* (AEY77130.1), *Argopecten irradians* (AAX09979.1), *Azumapecten farreri* (ABB53641.1).

rPmlysG treatment (shown by an arrow in [Figures 8D, E](#)). Meanwhile, plasmolysis was observed (shown by the arrow in [Figure 8F](#)), indicating that the cell wall collapse led to the release of local contents from the cell. The control group of *A. hydrophila* is shown in [Figures 8G–I](#). The cell appeared thin with a clear edge

and uniform content, whereas the bacterial cell wall was irregular in the experiment group of *Aeromonas hydrophila* ([Figure 8J](#)). Further magnification revealed that these two cell walls were dissolved, and the contents were lost in the hollow state (shown by an arrow in [Figures 8K–L](#)).

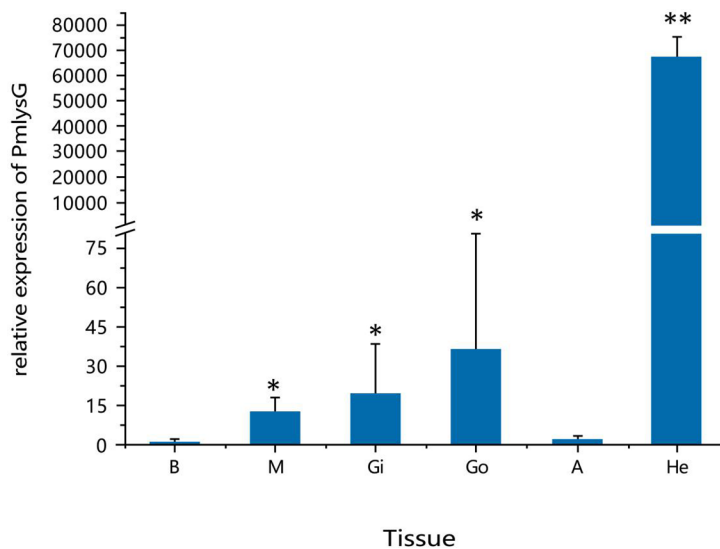


**FIGURE 4**  
 Quantitative analysis of *PmlysG* gene expression. He: Hepatopancreas, Gi: Gill, Go: Gonad, M: Mantle, H: hemocytes, A: Adductor muscle. \*,  $P < 0.05$ ; \*\*,  $P < 0.01$ .

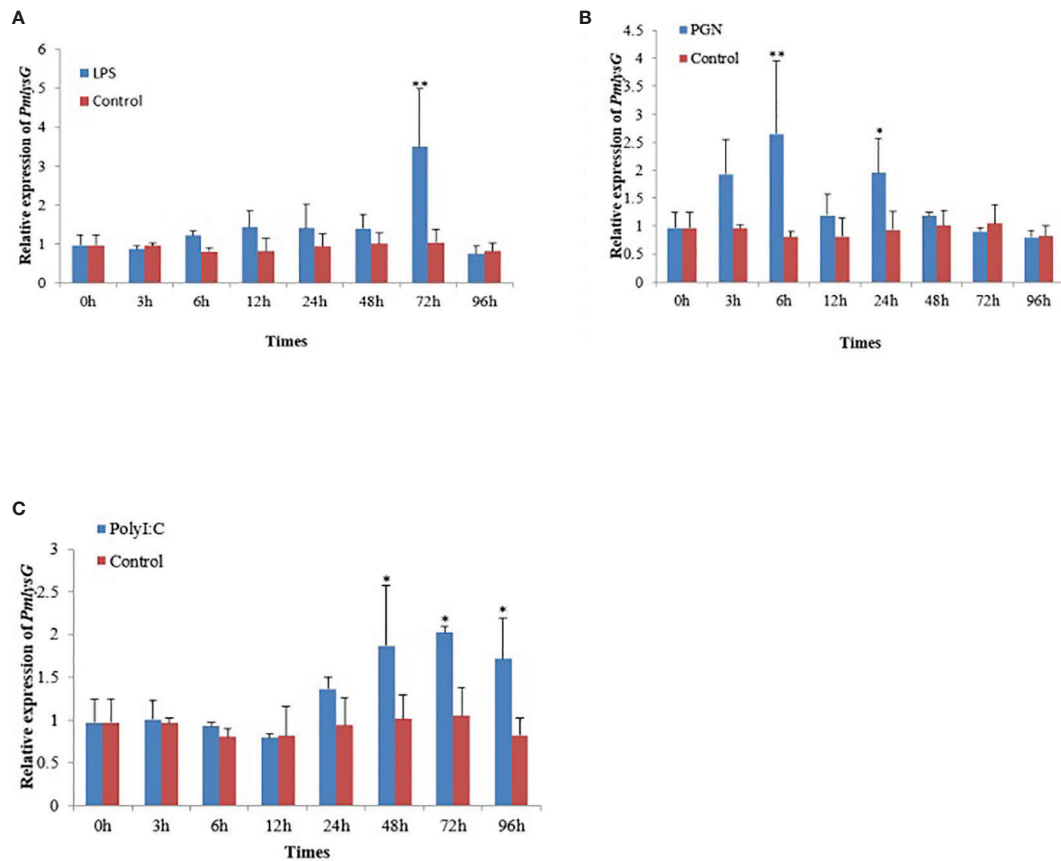


FIGURE 5

The *PmlysG* mRNA expression level in the hepatopancreas of *P.f. martensii* after PAMPs stimulation. (A) LPS stimulation, (B) PGN stimulation, (C) PolyI: C stimulation. The asterisks \*,  $P < 0.05$ , \*\*, and  $P < 0.01$  indicate significant differences between the control and stimulation groups. Vertical bars represent the mean  $\pm$  SD ( $n=5$ ).

## Discussion

Innate immunity is the first line of defense in marine invertebrates against pathogenic attacks (Wang et al., 2018; Cao et al., 2019). Lysozyme is a vital component of innate immunity and has been detected in body fluids and tissues of many bivalve scallops (McHenery and Birkbeck, 1982; Matsumoto et al., 2006). Besides, the g-type lysozymes have also been identified in vertebrates and some mollusks (Zhao et al., 2007). Therefore, studying the structure and immune characteristics of g-type lysozymes in *P.f. martensii* is of great significance. In this study, a g-type lysozyme gene, encoding a polypeptide with 255 amino acids, was isolated from *P.f. martensii*. Sequence analysis showed that the *PmlysG* gene contain a d153I\_domain. Following the alignment of domain structure and NCBI prediction, the protein was deduced to be a g-type lysozyme. The physical and chemical properties analysis revealed that *PmlysG* formed a signal peptide at positions 1-16 amino acids, indicating that *PmlysG* is a secretory protein. This

was consistent with the description of *Chlamys farreri* (Zhao et al., 2007) and gastropod *Oncomelania* (Zhang et al., 2012). All these species had a signal peptide, indicating the presence of secretory proteins (Irwin and Gong, 2003). It is likely that activation of *PmlysG* expression is a host immune defense directed against general bacterial invasion. Moreover, there was no transmembrane structure, indicating that the protein was not a transmembrane protein. In contrast, the signal peptide is not common in the g-type lysozymes of fish. Only a few fish g-type lysozymes have secretion signals, such as the g-type lysozymes from *Salmo sala* (Kyomuhendo et al., 2007), but lacks the disulfide bond and N-terminal signal peptide, which is consistent with the lysozymes from *C. idellus* (Yin et al., 2003), *Scophthalmus maximus* (Zhao et al., 2011), and *Epinephelus coioides* (Wei et al., 2014). *PmlysG* has three conserved catalytic sites (Glu, Asp, Asp), the critical involvement of Glu and Asp in the catalytic activity, also indicate that the Glu residue has pivotal role in the structural stability of G-type lysozyme (Hirakawa et al., 2008). It can promote G-type lysozyme

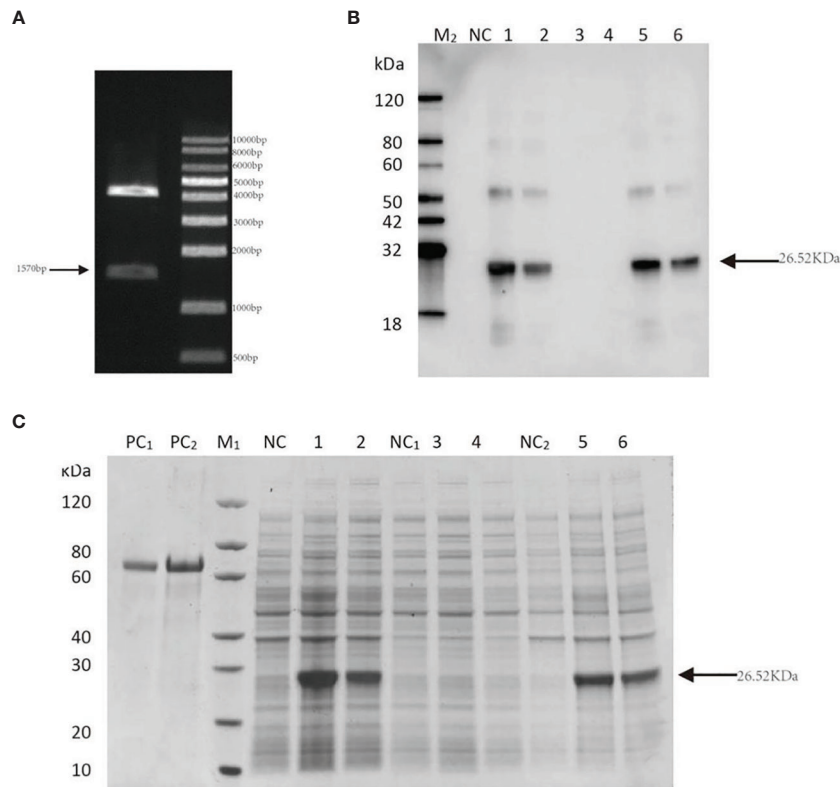


FIGURE 6

Construction of *PmlysG* recombinant protein. (A) Verification of recombinant plasmid of *PmlysG* 1: Bands of interest M: Maker. (B) SDS-PAGE (C) Western Blot. PC<sub>1</sub>: BSA (1 μg); PC<sub>2</sub>: BSA (2 μg); M<sub>1</sub>,M<sub>2</sub>: Marker; NC(whole bacteria): Cell lysate without induction; 1: Cell lysate with induction at 15°C for 16 hours; 2: Cell lysate with induction at 37°C for 4 hours; NC<sub>1</sub>(supernatant): Supernatant of cell lysate without induction; 3: Supernatant of cell lysate with induction at 15°C for 16 hours; 4: Supernatant of cell lysate with induction at 37°C for 4 hours; NC<sub>2</sub> (precipitation): Debris of cell lysate without induction; 5: Debris of cell lysate with induction at 15°C for 16 hours; 6: Debris of cell lysate with induction at 37°C for 4 hours.

catalyze the hydrolysis of the  $\beta$ -1,4-glycosidic linkage between N-acetylmuramic acid and N-acetylglucosamine alternating sugar residues in the bacterial cell walls and peptidoglycan. The crystal structures of GEL, free and complexed with (GlcNAc)<sub>3</sub>, revealed that the three-dimensional position of Glu73 in GEL is analogous to those of Glu35 in HEL and Glu11 in T4L, which are believed to act as a general acid to donate a proton to the glycosidic bond, thereby facilitating bond cleavage (Weaver et al., 1995; Kawamura et al., 2006).

Multiple sequence alignments showed that the g-type lysozymes of *PmlysG* had high similarity with other species, with the highest similarity in *Argopecten irradians* (60.5%), indicating that *PmlysG* maintains high conservatism during evolution. Evolutionary analysis showed that *P.f. martensii* could cluster with *Argopecten irradians*, *Azumapecten farreri*, and *Mizuhopecten yessoensis*, consistent with the relationship of species evolution.

Therefore, assessing the functional characteristics of *PmlysG* is highly necessitated. Herein, the qRT-PCR analysis showed

that *PmlysG* mRNA was expressed in all tissues. Moreover, the mRNA expression was the highest in hepatopancreas compared with other tissues. Previous studies have detected lysozyme activity in the hepatopancreas of several marine bivalves. The mRNA expression level of *Meretrix meretrix* was higher in the hepatopancreas than in other tissues (Yue et al., 2011). The high expression level of *PmlysG* mRNA in the hepatopancreas indicate that it is the primary site for the synthesis of g-type lysozymes. These results confirm that *PmlysG* is a digestive enzyme that can protect digestive organs from bacterial attacks. Digestive lysozymes may have a potentially low pH and isoelectric points and higher resistance to proteases (Callewaert and Michiels, 2010).

After LPS stimulation, the mRNA expression level of *PmlysG* reached a maximum at 72 hours. After PGN stimulation, the mRNA expression level of *PmlysG* reached a maximum at 6 hours, then increased for the second time at 48 hours. After PolyI:C stimulation, the mRNA expression level of *PmlysG* reached a maximum at 72 hours. Although the three

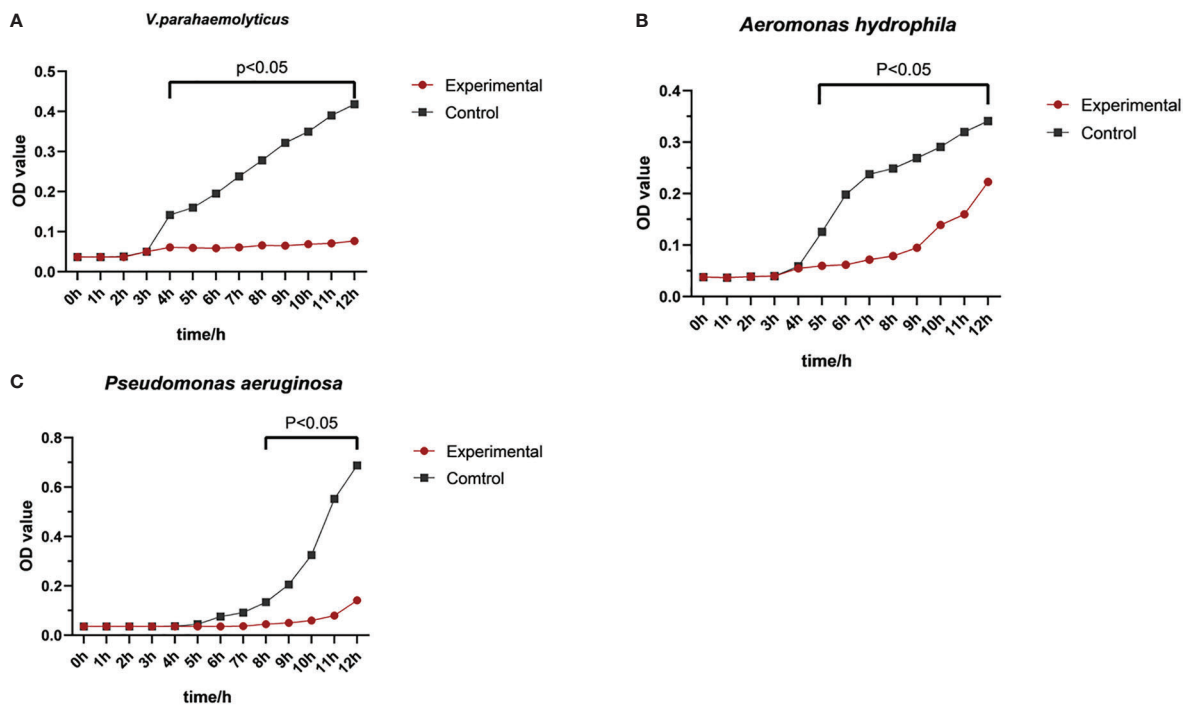


FIGURE 7  
Antibacterial activity of rPmlysG. Control group: PBS. Experimental groups; (A) *V. parahaemolyticus* challenge; (B) *A. hydrophila* challenge; (C) *Pseudomonas aeruginosa* challenge.

stimulation modes mediated immune response, they had different effects with time. For instance, the mRNA expression was the highest at 72 hours after LPS and PolyI:C stimulation, suggesting that *PmlysG* might be less involved in the immune response of pathogens containing LPS and PolyI:C in the early stage. Similarly, the mRNA expression was maximum at 6 hours after PGN stimulation, indicating that *PmlysG* might quickly participate in the immune defense of PGN model pathogens. These results were consistent with the g-type lysozymes of other species stimulated with PAMPs. For instance, *PalysG* identified in *Physa acuta* could sustain high expression in the hepatopancreas within 8–48 hours after LPS stimulation (Guo and He, 2014). *CalysG* identified in *Carassius auratus* could sustain high expression in the hepatopancreas within 6–48 hours after LPS stimulation (Wang et al., 2016). These results show that *PmlysG* has various biological functions, and it is a multifunctional molecule essential for digestive function and host immune response.

The rPmlysG was used to identify the antibacterial properties. Several studies have indicated that some g-type lysozymes could inhibit microbial growth. For instance, a g-type lysozyme isolated from *Chlamys farreri* (Zhao et al., 2007) (rCFlysG) can inhibit *V. parahaemolyticus*, *V. splendidus*, and *V. anguillarum*. Similarly, a g-type lysozyme of salmon can inhibit

the growth of *Aeromonas hydrophila* (Zhang et al., 2018). The recombinant g-type lysozyme of grass carp can inhibit *A. hydrophila*, *V. parahaemolyticus*, and *Bacillus cereus* (Ye et al., 2010; Yang et al., 2016). Additionally, rPmlysG showed potent lytic activity against *V. parahaemolyticus*, *A. hydrophila*, and *Pseudomonas aeruginosa*. However, the activity was less for gram-positive bacteria. Studies have reported that the antimicrobial action occurs through the hydrolysis of  $\beta$ -1,4-glycosidic linkage between N-acetylmuramic acid and N-acetylglucosamine alternating the sugar residues in the PGN of bacterial cell walls, thereby inducing bacterial cell lysis (Mohapatra et al., 2019). In this study, rPmlysG damaged the cell wall of *V. parahaemolyticus* and *A. hydrophila*, inducing the release of bacterial contents. This attack pattern was consistent with the Chitosan-lysozyme nanoparticles (CS-Lys-NPs) (Wu et al., 2017c). This experiment provides insights into immunological research and disease control in *P.f. martensii*.

## Conclusion

In this study, a g-type lysozyme gene was successfully cloned from *P.f. martensii*. The amino acid sequence of *PmlysG* shared a

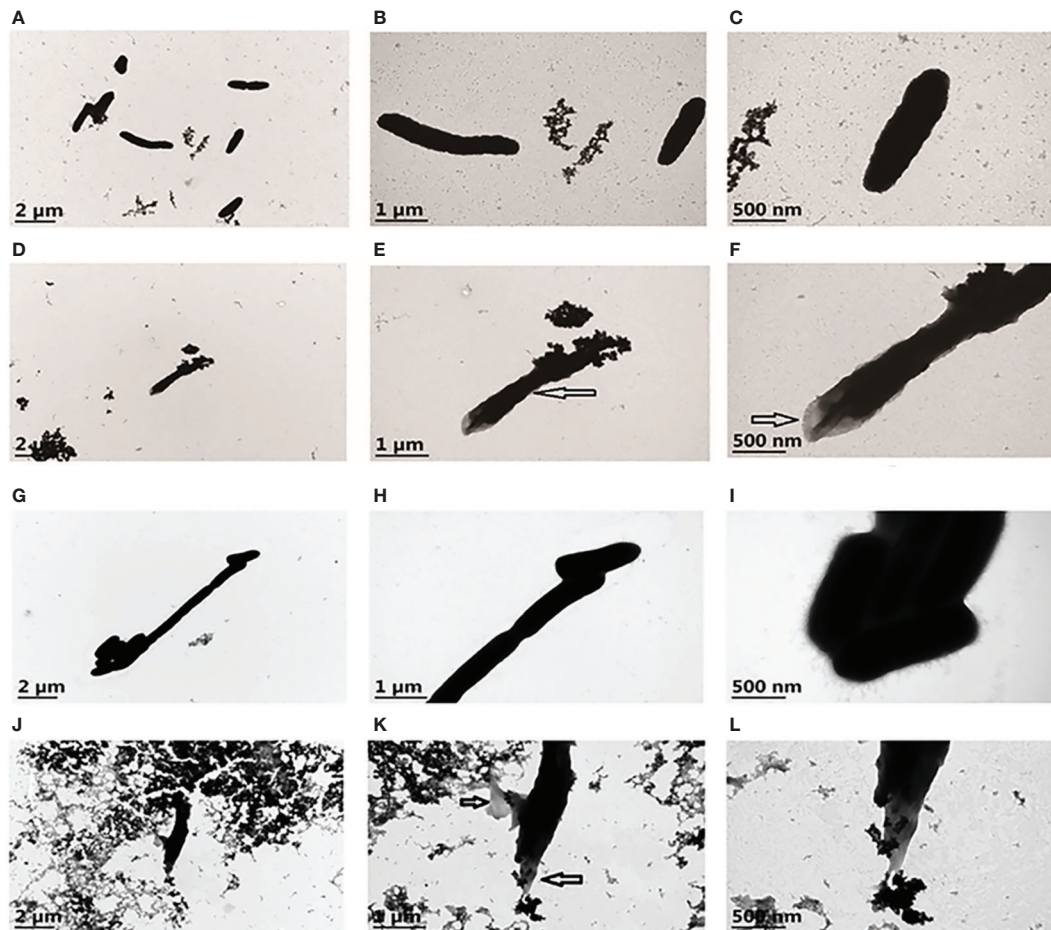


FIGURE 8

Transmission Electron Microscopy of *V. parahaemolyticus* and *A. hydrophila* untreated and treated with rPmlysG. (A) The control group of *V. parahaemolyticus* untreated with rPmlysG; (B, C) represent enlarged views of A; (D) *V. parahaemolyticus* action with rPmlysG; (E, F) represent enlarged views of D; (G) The control group of *A. hydrophila* untreated with rPmlysG; (H, I) represent enlarged views of G; (J) *A. hydrophila* action with rPmlysG; (K, L) represent enlarged views of J.

high similarity with other known shellfish. The mRNA expression analysis indicated that *PmlysG* was highly expressed in the hepatopancreas. PAMPs stimulation induced an immune response in the body, and rPmlysG exhibited significant antibacterial activity. Overall, these results confirm that the g-type lysozyme plays a key role in the innate immunity of *P.f. martensii*.

## Data availability statement

The datasets presented in this study can be found in online repositories. The names of the repository/repositories and accession number(s) can be found in the article/ [Supplementary Material](#).

## Author contributions

ZG: Investigation and designed the study, Analyzed all data, Writing - Original draft preparation. CS: Analyzed all sequencing data. HL: Conceptualization, Methodology, Writing- Reviewing and Editing. MZ: Prepared the samples, Analyzed all sequencing data. BL: Conclusion. BZ: Prepared the samples, Formal analysis. All authors contributed to the article and approved the submitted version.

## Funding

This work was supported by the grants from the National Natural Science Foundation of China (No. 31472306),

Guangdong Natural Science Foundation of China (No. 2021A1515010962), Science and technology Special Fund of Guangdong Province (2021A05250), Special Fund for Harbor Construction and Fishery Industry Development of Guangdong Province (No. A201608B15) and Sustainable Development Project of Shenzhen Science and Technology Program (KCXFZ20211020165547010).

## Conflict of interest

The authors declare that the research was conducted in the absence of any commercial or financial relationships that could be construed as a potential conflict of interest.

## References

- Callewaert, L., and Michiels, C. W. (2010). Lysozymes in the animal kingdom. *J. Biosci.* 35 (1), 127–160. doi: 10.1007/s12038-010-0015-5
- Canfield, R. E., and McMurry, S. (1967). Purification and characterization of a lysozyme from goose egg white. *Biochem. Biophys. Res. Commun.* 26 (1), 38–42. doi: 10.1016/0006-291x(67)90249-5
- Cao, Y., Yang, S., Feng, C., Zhan, W., Zheng, Z., Wang, Q., et al. (2019). Evolution and function analysis of interleukin-17 gene from *Pinctada fucata martensii*. *Fish Shellfish Immunol.* 88, 102–110. doi: 10.1016/j.fsi.2019.02.044
- Du, X., Fan, G., Jiao, Y., Zhang, H., Guo, X., Huang, R., et al. (2017). The pearl oyster *pinctada fucata martensii* genome and multi-omic analyses provide insights into biomineralization. *Gigascience* 6 (8), 1–12. doi: 10.1093/gigascience/gix059
- Fan, S., Wang, W., Li, J., Cao, W., Li, Q., Wu, S., et al. (2022). The truncated MyD88s negatively regulates TLR2 signal on expression of IL17-1 in oyster *Crassostrea gigas*. *Dev. Comp. Immunol.* 133, 104446. doi: 10.1016/j.dci.2022.104446
- Guo, Y., and He, H. (2014). Identification and characterization of a goose-type lysozyme from sewage snail *Physa acuta*. *Fish Shellfish Immunol.* 39 (2), 321–325. doi: 10.1016/j.fsi.2014.05.029
- Hancock, R. E., and Scott, M. G. (2000). The role of antimicrobial peptides in animal defenses. *Proc. Natl. Acad. Sci. U.S.A.* 97 (16), 8856–8861. doi: 10.1073/pnas.97.16.8856
- He, J., Liang, H., Wu, Y., and Deng, Y. (2018). Gene cloning and tissue expression analysis of adapter protein 368 CIKS from *Pinctada fucata martensii*. *J. Guangdong Ocean Univ.* 38 (4), 369 1–7. doi: 10.3969/j.issn.1673-9159.2018.04.001
- He, J., Liang, H., Zhu, J., and Fang, X. (2019). Separation, identification and gene expression analysis of PmAMP-1 from *Pinctada fucata martensii*. *Fish Shellfish Immunol.* 92, 728–735. doi: 10.1016/j.fsi.2019.07.002
- He, J., Shen, C., Liang, H., Fang, X., and Lu, J. (2020). Antimicrobial properties and immune-related gene expression of a c-type lectin isolated from *Pinctada fucata martensii*. *Fish Shellfish Immunol.* 105, 330–340. doi: 10.1016/j.fsi.2020.07.017
- He, C., Yu, H., Liu, W., Su, H., Shan, Z., Bao, X., et al. (2012). A goose-type lysozyme gene in Japanese scallop (*Mizuhopecten yessoensis*): cDNA cloning, mRNA expression and promoter sequence analysis. *Comp. Biochem. Physiol. Part B: Biochem. Mol. Biol.* 162 (1), 34–43. doi: 10.1016/j.cbpb.2012.02.002
- Hikima, J.-i., Minagawa, S., Hirono, I., and Aoki, T. (2001). Molecular cloning, expression and evolution of the Japanese flounder goose-type lysozyme gene, and the lytic activity of its recombinant protein. *Biochim. Biophys. Acta (BBA) - Gene Structure Expression* 1520 (1), 35–44. doi: 10.1016/S0167-4781(01)00248-2
- Hirakawa, H., Ochi, A., Kawahara, Y., Kawamura, S., Torikata, T., and Kuhara, S. (2008). Catalytic reaction mechanism of goose egg-white lysozyme by molecular modelling of enzyme-substrate complex. *J. Biochem.* 144 (6), 753–761. doi: 10.1093/jb/mvn133
- Irwin, D. M., and Gong, Z. M. (2003). Molecular evolution of vertebrate goose-type lysozyme genes. *J. Mol. Evol.* 56 (2), 234–242. doi: 10.1007/s00239-002-2396-z
- Jiménez-Cantizano, R. M., Infante, C., Martín-Antonio, B., Ponce, M., Hachero, I., Navas, J. I., et al. (2008). Molecular characterization, phylogeny, and expression of c-type and g-type lysozymes in brill (*Scophthalmus rhombus*). *Fish Shellfish Immunol.* 25 (1), 57–65. doi: 10.1016/j.fsi.2007.12.009
- Jollès, P., and Jollès, J. (1984). What's new in lysozyme research? always a model system, today as yesterday. *Mol. Cell Biochem.* 63 (2), 165–189. doi: 10.1007/bf00285225
- Kawamura, S., Ohno, K., Ohkuma, M., Chijiwa, Y., and Torikata, T. (2006). Experimental verification of the crucial roles of Glu73 in the catalytic activity and structural stability of goose type lysozyme. *J. Biochem.* 140 (1), 75–85. doi: 10.1093/jb/mvj125
- Kyomuhendo, P., Myrnes, B., and Nilsen, I. W. (2007). A cold-active salmon goose-type lysozyme with high heat tolerance. *Cell. Mol. Life Sci. CMLS* 64 (21), 2841–2847. doi: 10.1007/s00018-007-7372-8
- Liang, H., Zhang, M., Shen, C., He, J., Lu, J., and Guo, Z. (2022). Cloning and functional analysis of a trypsin-like serine protease from *Pinctada fucata martensii*. *Fish Shellfish Immunol.* 126, 327–335. doi: 10.1016/j.fsi.2022.05.058
- Li, H., Parisi, M.-G., Toubiana, M., Cammarata, M., and Roch, P. (2008). Lysozyme gene expression and hemocyte behaviour in the Mediterranean mussel, *mytilus galloprovincialis*, after injection of various bacteria or temperature stresses. *Fish Shellfish Immunol.* 25 (1), 143–152. doi: 10.1016/j.fsi.2008.04.001
- Livak, K. J., and Schmittgen, T. D. (2001). Analysis of relative gene expression data using real-time quantitative PCR and the 2<sup>-delta delta C(T)</sup> method. *Methods* 25 (4), 402–408. doi: 10.1006/meth.2001.1262
- Li, L., Zhao, J., Wang, L., Qiu, L., and Song, L. (2013). Genomic organization, polymorphisms and molecular evolution of the goose-type lysozyme gene from zhikong scallop *Chlamys farreri*. *Gene* 513 (1), 40–52. doi: 10.1016/j.gene.2012.10.080
- Lu, J., Zhang, M., Liang, H., Shen, C., Zhang, B., Liang, B., et al. (2022). Comparative proteomics and transcriptomics illustrate the allograft-induced stress response in the pearl oyster (*Pinctada fucata martensii*). *Fish Shellfish Immunol.* 121 (74), 85. doi: 10.1016/j.fsi.2021.12.055
- Lv, X., Yang, W., Guo, Z., Wu, W., Li, Y., Yan, X., et al. (2022). CgHMGB1 functions as a broad-spectrum recognition molecule to induce the expressions of CgIL17-5 and Cgdefh2 via MAPK or NF-κB signaling pathway in *Crassostrea gigas*. *Int. J. Biol. Macromol.* 211, 289–300. doi: 10.1016/j.ijbiomac.2022.04.166
- Matsumoto, T., Nakamura, A. M., and Takahashi, K. G. (2006). Cloning of cDNAs and hybridization analysis of lysozymes from two oyster species, *Crassostrea gigas* and *Ostrea edulis*. *Comp. Biochem. Physiol. Part B: Biochem. Mol. Biol.* 145 (3), 325–330. doi: 10.1016/j.cbpb.2006.08.003
- McHenry, J. G., and Birkbeck, T. H. (1982). Characterization of the lysozyme of *Mytilus edulis* (L.). *Comp. Biochem. Physiol. B* 71 (4), 583–589. doi: 10.1016/0305-0491(82)90466-7

## Publisher's note

All claims expressed in this article are solely those of the authors and do not necessarily represent those of their affiliated organizations, or those of the publisher, the editors and the reviewers. Any product that may be evaluated in this article, or claim that may be made by its manufacturer, is not guaranteed or endorsed by the publisher.

## Supplementary material

The Supplementary Material for this article can be found online at: <https://www.frontiersin.org/articles/10.3389/fmars.2022.1012323/full#supplementary-material>

- Mohapatra, A., Parida, S., Mohanty, J., and Sahoo, P. K. (2019). Identification and functional characterization of a g-type lysozyme gene of *Labeo rohita*, an Indian major carp species. *Dev. Comp. Immunol.* 92, 87–98. doi: 10.1016/j.dci.2018.11.004
- Nilsen, I. W., Myrnes, B., Edvardsen, R. B., and Chourrout, D. (2003). Urochordates carry multiple genes for goose-type lysozyme and no genes for chicken- or invertebrate-type lysozymes. *Cell. Mol. Life Sci. CMLS* 60 (10), 2210–2218. doi: 10.1007/s00018-003-3252-z
- Nilsen, I. W., Overbø, K., Sandsdalen, E., Sandaker, E., Sletten, K., and Myrnes, B. (1999). Protein purification and gene isolation of chlamysin, a cold-active lysozyme-like enzyme with antibacterial activity. *FEBS Lett.* 464 (3), 153–158. doi: 10.1016/s0014-5793(99)01693-2
- Prager, E. M., and Jollès, P. (1996). Animal lysozymes c and g: an overview. *Exs* 75, 9–31. doi: 10.1007/978-3-0348-9225-4\_2
- Qiu, Y., Lu, H., Zhu, J., Chen, X., Wang, A., and Wang, Y. (2014). Characterization of novel EST-SSR markers and their correlations with growth and nacreous secretion traits in the pearl oyster *Pinctada martensii* (Dunker). *Aquaculture* 420–421, S92–S97. doi: 10.1016/j.aquaculture.2013.09.040
- Rolf, J., and Siva-Jothy, M. T. (2003). Invertebrate ecological immunology. *Science* 301 (5632), 472–475. doi: 10.1126/science.1080623
- Shakoori, M., Hoseiniifar, S. H., Paknejad, H., Jafari, V., Safari, R., Van Doan, H., et al. (2019). Enrichment of rainbow trout (*Oncorhynchus mykiss*) fingerlings diet with microbial lysozyme: Effects on growth performance, serum and skin mucus immune parameters. *Fish Shellfish Immunol.* 86, 480–485. doi: 10.1016/j.fsi.2018.11.077
- Wang, L., Qiu, L., Zhou, Z., and Song, L. (2013). Research progress on the mollusc immunity in China. *Dev. Comp. Immunol.* 39 (1), 2–10. doi: 10.1016/j.dci.2012.06.014
- Wang, L., Song, X., and Song, L. (2018). The oyster immunity. *Dev. Comp. Immunol.* 80, 99–118. doi: 10.1016/j.dci.2017.05.025
- Wang, M., Zhao, X., Kong, X., Wang, L., Jiao, D., and Zhang, H. (2016). Molecular characterization and expressing analysis of the c-type and g-type lysozymes in qihе crucian carp *Carassius auratus*. *Fish Shellfish Immunol.* 52, 210–220. doi: 10.1016/j.fsi.2016.03.040
- Weaver, L. H., Grütter, M. G., and Matthews, B. W. (1995). The refined structures of goose lysozyme and its complex with a bound trisaccharide show that the “goose-type” lysozymes lack a catalytic aspartate residue. *J. Mol. Biol.* 245 (1), 54–68. doi: 10.1016/s0022-2836(95)80038-7
- Wei, S., Huang, Y., Huang, X., Cai, J., Wei, J., Li, P., et al. (2014). Molecular cloning and characterization of a new G-type lysozyme gene (Ec-lysG) in *orange-spotted grouper*, *epinephelus coioides*. *Dev. Comp. Immunol.* 46 (2), 401–412. doi: 10.1016/j.dci.2014.05.006
- Wu, Y., Guo, Z., and Liang, H. (2017c). Clone and expression analysis of PmLec-8 gene from *Pinctada fucata martensii*. *J. Guangdong Ocean Univ.* 37 (04), 1–7. doi: 10.3969/j.issn.1673-9159.2017.04.001
- Wu, Y., Liang, H., Wang, Z., Lei, Q., and Xia, L. (2017b). A novel toll-like receptor from the pearl oyster *pinctada fucata martensii* is induced in response to stress. *Comp. Biochem. Physiol. Part B: Biochem. Mol. Biol.* 214, 19–26. doi: 10.1016/j.cbpb.2017.08.006
- Wu, T., Wu, C., Fu, S., Wang, L., Yuan, C., Chen, S., et al. (2017a). Integration of lysozyme into chitosan nanoparticles for improving antibacterial activity. *Carbohydr. Polymers* 155, 192–200. doi: 10.1016/j.carbpol.2016.08.076
- Yang, Y., Yu, H., Li, H., and Wang, A. (2016). Transcriptome profiling of grass carp (*Ctenopharyngodon idellus*) infected with *aeromonas hydrophila*. *Fish Shellfish Immunol.* 51, 329–336. doi: 10.1016/j.fsi.2016.02.035
- Ye, X., Zhang, L., Tian, Y., Tan, A., Bai, J., and Li, S. (2010). Identification and expression analysis of the g-type and c-type lysozymes in grass carp *Ctenopharyngodon idellus*. *Dev. Comp. Immunol.* 34 (5), 501–509. doi: 10.1016/j.dci.2009.12.009
- Yin, Z. X., He, J. G., Deng, W. X., and Chan, S. M. (2003). Molecular cloning, expression of orange-spotted grouper goose-type lysozyme cDNA, and lytic activity of its recombinant protein. *Dis. Aquat. Organ.* 55 (2), 117–123. doi: 10.3354/dao055117
- Yue, X., Liu, B., and Xue, Q. (2011). An i-type lysozyme from the Asiatic hard clam *meretrix meretrix* potentially functioning in host immunity. *Fish Shellfish Immunol.* 30 (2), 550–558. doi: 10.1016/j.fsi.2010.11.022
- Zhang, C., Zhang, J., Liu, M., and Huang, M. (2018). Molecular cloning, expression and antibacterial activity of goose-type lysozyme gene in *Micropterus salmoides*. *Fish Shellfish Immunol.* 82, 9–16. doi: 10.1016/j.fsi.2018.07.058
- Zhang, S. H., Zhu, D. D., Chang, M. X., Zhao, Q. P., Jiao, R., Huang, B., et al. (2012). Three goose-type lysozymes in the gastropod *Oncomelania hupensis*: cDNA sequences and lytic activity of recombinant proteins. *Dev. Comp. Immunol.* 36 (1), 241–246. doi: 10.1016/j.dci.2011.06.014
- Zhao, J., Song, L., Li, C., Zou, H., Ni, D., Wang, W., et al. (2007). Molecular cloning of an invertebrate goose-type lysozyme gene from *Chlamys farreri*, and lytic activity of the recombinant protein. *Mol. Immunol.* 44 (6), 1198–1208. doi: 10.1016/j.molimm.2006.06.008
- Zhao, L., Sun, J.-s., and Sun, L. (2011). The g-type lysozyme of *scophthalmus maximus* has a broad substrate spectrum and is involved in the immune response against bacterial infection. *Fish Shellfish Immunol.* 30 (2), 630–637. doi: 10.1016/j.fsi.2010.12.012
- Zheng, W., Tian, C., and Chen, X. (2007). Molecular characterization of goose-type lysozyme homologue of large yellow croaker and its involvement in immune response induced by trivalent bacterial vaccine as an acute-phase protein. *Immunol. Lett.* 113 (2), 107–116. doi: 10.1016/j.imlet.2007.08.001